

**Computer Science Department Technical Report
University of California
Los Angeles, CA 90024-1596**

**EXCITATION WAVE PROPAGATION ALONG NARROW
PATHWAYS, UNIDIRECTIONAL BLOCK AND
REENTRY (THEORETICAL STUDY)**

**Boris Y. Kogan
Walter J. Karplus
Brian S. Billet**

**July 1991
CSD-910053**

**EXCITATION WAVE PROPAGATION
ALONG NARROW PATHWAYS,
UNIDIRECTIONAL BLOCK AND REENTRY
(THEORETICAL STUDY)**

Boris Y. Kogan, Walter J. Karplus, Brian S. Billett

JULY 16, 1991

TECHNICAL REPORT # 910053

**COMPUTER SCIENCE DEPARTMENT
UNIVERSITY OF CALIFORNIA
LOS ANGELES**

Excitation Wave Propagation Along Narrow Pathways, Unidirectional Block and Reentry (Theoretical study)

Boris Y. Kogan, Walter J. Karplus, Brian S. Billett
Computer Science Department, UCLA

Abstract

Reentrant arrhythmias are common in a diseased myocardium where regions of normal tissue are interspersed with inexcitable ones. We hypothesize that reentry may occur due to unidirectional block caused solely by variations in the pathway geometry of survival tissue in the diseased myocardium. To determine the exclusive role of pathway geometry, two idealized cases are considered: propagation through narrow paths with parallel and tapered borders. Borders can be of two types: "zero flux" and diminished excitability. Using the relationship between stationary speed of wave front propagation and its curvature, it is shown that unidirectional block can occur in narrow paths with parallel borders with "zero flux" boundary conditions when the wave leaves the narrow path and emerges into an open area of appropriate size. In narrow paths with parallel borders of low excitable tissue, unidirectional blocks are impossible. For this situation, the wave blocked or propagated in both directions inside the pathway depending on its width. The size of the opening for this case has no effect on the occurrence of unidirectional block. Unidirectional block occurs only when the narrow path has the proper tapered shape. Waves propagating from the wide end of the pathway die out at narrow end, while waves propagating in the opposite direction are able to pass through. It is shown for both types of border conditions that the arrangement of several pathways in parallel, joined by a common space of a vital tissue, permits the appearance of reentry. For this purpose it is necessary that at least one pathway should have a geometry that provides unidirectional block and that cells inside the channel with unidirectional block have sufficient time to recover from the previous excitation. The latter is facilitated by the anisotropy properties of heart muscle tissue.

1. Introduction

Reentrant arrhythmias are observed in originally normal hearts after appropriate application of premature beats (Winfree [1], Ideker et.al[2]) and in diseased tissue during different stages of the development of myocardium infarction (MI) when regions of normal tissue are interspersed with ischemic regions (Janse and Wit [3]). In the latter case, the arrangement of healthy and diseased tissues creates paths of varied, and some times very complicated, forms. The histology of the surviving areas in the infarct zone (DeBakker et.al. [4]) shows vital muscle bundles alternated by zones of connective tissue. The surviving bundles vary markedly in size and shape, and occasionally these bundles merge and bifurcate and abruptly exit to a region with a big mass of healthy tissue. More - over the borders of these paths may have different properties depending on the time elapsed after the MI occurrence. The cells in these regions may be surrounded by nonexcitable connective tissue, and by tissue with decreased excitability and significantly increased coupling (gap) resistance. Anisotropy of heart muscle tissue also plays an important

role in the establishment of reentry (Cardinal et.al. [5], Wit [6], Dillon et.al. [7]).

The investigation that forms the subject of this paper was undertaken to find the explanation for the induced reentrant arrhythmia in the presence of MI scars and to relate this phenomenon to pathway geometry. The pathway geometry and border conditions determine the shape of propagated wave front and its curvature. The theory of traveling waves provide the relationship between the stationary speed of wave propagation and the curvature of the wave front. Here we briefly describe the basic idea used to derive this relationship. In order to facilitate the investigation, two idealized cases are considered: propagation through narrow paths with smooth parallel and tapered borders. More complicated pathway configurations can be considered as various combinations of these two. It is assumed that the dimensions of narrow paths are considerably bigger than that of the cell. This allows us to limit the study to macroprocesses. The results of microscopic studies are described in Spach et.al [8], Rudy and Quan [9]. Two types of border conditions are considered in this paper: "zero flux" border condition ($\frac{\partial E}{\partial n}=0$, E - membrane potential, n - direction of the normal to the border) and borders with decreased excitability. The case when borders cells have significantly increased coupling resistance can be approximated by the zero flux condition.

All computer simulation results are combined in a separate report. They affirm the correctness of the assumptions made in the course of theoretical study and extend the study to a number of additional cases. These results were obtained using a previously developed computer simulation approach (Kogan et.al. [10]) using the the massively parallel computer system: Connection Machine - 2 (CM). The modified FitzHugh-Nagumo equations which include the action potential duration restitution properties (Kogan et.al.[11]) are implemented on the CM by creating a grid of 128x128 nodes. A new numerical integration algorithm proposed in Ashour and Hanna [12] for mildly stiff integration is used to decrease the overall time of calculation.

2. The dependence of stationary speed of propagation on wave front curvature

The relationship between the speed of 2D stationary wave propagation and front curvature was obtained first by Zykov [13] and then by Tyson and Keener [14]. Here we remind the reader briefly of these results for isotropic excitable media with respect to the simplified FH-N model, emphasizing the specific assumptions

for which they are valid; to modify the model for anisotropic tissue and use it to further investigations of wave propagation along narrow paths.

2.1. Isotropic tissue

For isotropic tissue, the diffusion coefficients are the same in the directions of the fiber's longitudinal axis x , and along the transverse axis y : $D_x=D_y=D$. Therefore, the simplified FH-N equations have the form:

$$D \left(\frac{\partial^2 E}{\partial x^2} + \frac{\partial^2 E}{\partial y^2} \right) = c \frac{\partial E}{\partial t} - F(E) + I - I_{st} \quad (1)$$

$$\frac{\partial I}{\partial t} = \epsilon(E)(G_s E - I) \quad (2)$$

Here :

E - transmembrane potential [mV]

I - generalized outward current [$\frac{mA}{cm^2}$]

t - time [msec]

D - diffusion coefficient [$\frac{1}{cm}$]

c - membrane electrical capacity [$\frac{\mu F}{cm^2}$]

x, y - space coordinates [cm]

$F(E)$ - fast inward current-voltage characteristic represented as a piecewise linear approximation of a cubic parabola

$\epsilon(E)$ - small parameter inversely proportional to the value of time constant of the slow outward current. The continuous function $\epsilon(E)$ is represented by its piecewise step approximation

G_s - const. [$\frac{Om^{-1}}{cm^2}$]

The value of the local current at a given point on the wavefront is determined by the Laplacian in eqn.(1). The latter can be transformed to another form in order to introduce explicitly the influence of wavefront curvature K . For this purpose let us take advantage of well known identity:

$$\frac{\partial^2 E}{\partial x^2} + \frac{\partial^2 E}{\partial y^2} = \text{div } \nabla E$$

Using vector analysis, this identity can be rewritten as :

$$\text{div } \nabla E = (\mathbf{n}, \text{grad}(\text{grad} E, \mathbf{n})) + (\text{grad} E, \mathbf{n}) \text{div } \mathbf{n}$$

where (\mathbf{A}, \mathbf{B}) denotes the scalar product of vector \mathbf{A} and \mathbf{B}

Let us introduce the curvilinear coordinate z , oriented in the direction of the current flow (which is normal to the level lines of E). The scalar products of the right-hand side of the above equation can be represented in the form:

$$(\text{grad} E, \mathbf{n}) = -\frac{\partial E}{\partial z}; (\mathbf{n}, \text{grad}(\text{grad} E, \mathbf{n})) = \frac{\partial^2 E}{\partial z^2}$$

The components of the $\text{div } \mathbf{n} = \frac{\partial n_x}{\partial x} + \frac{\partial n_y}{\partial y}$ can be expressed in terms of the curvature K , using the relevant formula of differential geometry. So we finally obtain:

$$\frac{\partial^2 E}{\partial x^2} + \frac{\partial^2 E}{\partial y^2} = \frac{\partial^2 E}{\partial z^2} + K \frac{\partial E}{\partial z} \quad (3)$$

Here $K < 0$ for a convex front and $K > 0$ for a concave front.

Substituting (3) in (1), we reduce the problem to one dimension:

$$D \left(\frac{\partial^2 E}{\partial z^2} + K \frac{\partial E}{\partial z} \right) = c \frac{\partial E}{\partial t} - F(E) + I - I_{st} \quad (4)$$

$$\frac{\partial I}{\partial t} = \varepsilon (G_s E - I) \quad (5)$$

In system of eqn. (4), (5) the curvature K in the general case depends on the coordinate z along the current line and time t . For stationary wave propagation, however, the curvature K is constant along the front and does not change with time. For this particular case it is possible to simplify eqn. (4,5) further by introducing the transformation of variables $\xi = z + \theta t$; where θ denotes the propagation velocity, which for stationary propagation remains constant,

$$D \left(\frac{d^2 E}{d\xi^2} \right) = c \left(\theta - \frac{D}{c} K \right) \frac{dE}{d\xi} - F(E) + I + I_{st} \quad (6)$$

$$\theta \frac{dI}{d\xi} = \varepsilon (G_s E - I) \quad (7)$$

Equations (6,7) allow one to determine the stationary propagation velocity θ of the front wave segments with a given curvature K . For this purpose, the well-known and efficient numerical method proposed by Hodgkin and Huxley [15], and by Nagumo et al. [16] can be used. This method consists of multiple numerical integrations of the system (6,7) for a given K and constant initial conditions chosen

near the initial stationary state, but with different values of θ . Depending on the value of θ , the solution $E(\xi)$, as $\xi \rightarrow \infty$, tends either to $+\infty$ or $-\infty$. The velocity, θ , is determined computationally from the relation $\theta = \frac{\theta_+ + \theta_-}{2}$, where $\{\theta \text{ sub } +\}$ and $\{\theta \text{ sub } -\}$ are two closely spaced values of θ for which the solution diverge to $+\infty$ and $-\infty$ respectively. The results of numerical computations done by this method are presented in Fig.1 due to Zykov [17] for eqns (6,7) with standard set of parameters.

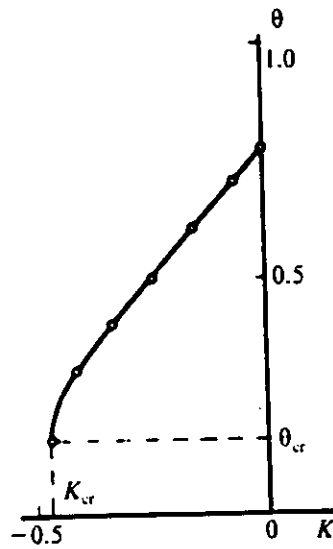


Figure 1. Dependence of the stationary wave propagation rate on wave front curvature.

These data manifest the following properties: the stationary propagation velocity decreases with increases absolute value of negative wave front curvature; there exists a curvature critical value beyond which propagation becomes impossible; and the critical curvature and corresponding critical speed of propagation are characteristics of any type of mathematical model and real excitable tissue.

A different approach is based on the reduction of equations (6,7) to a form similar to that when $K = 0$. For this purpose let us multiply eqn.(7) by the expression $(\theta - \frac{D}{c}K) \frac{1}{\theta}$ and modify eqn. (6) and (7) as:

$$\theta^* = \left(\theta - \frac{D}{c}K\right) \quad (8)$$

$$\varepsilon^* = \varepsilon \left(\theta - \frac{D}{c}K\right) \frac{1}{\theta} \quad (9)$$

Using this transformation of eqn. (6,7) we obtain:

$$D \frac{d^2 E}{d\xi^2} = c \theta^* \frac{dE}{d\xi} - F(E) + I$$

$$\theta^* \frac{dI}{d\xi} = \varepsilon^* (G_s E - I)$$

This system does not explicitly contain the curvature K and therefore can be considered as a system describing rectilinear wave propagation:

$$\theta^* = \theta_{rl}(\varepsilon^*) \quad (10)$$

Assuming that ε^* is small,

$$\theta_{rl}(\varepsilon^*) = \theta_0 + \theta_1 \varepsilon^* \quad (11)$$

Introducing eqn. (8), (9), and (11) in (10) and solving for θ ,

$$\theta = \frac{1}{2} \left(\theta_0 + \theta_1 \varepsilon + \frac{D}{c}K\right) + \frac{1}{2} \left[\left(\theta_0 + \theta_1 \varepsilon + \frac{D}{c}K\right)^2 - 4\theta_1 \varepsilon \frac{D}{c}K \right]^{\frac{1}{2}} \quad (12)$$

θ in eqn. (12) is real if:

$$\left(\theta_0 + \theta_1 \varepsilon + \frac{D}{c}K\right)^2 - 4\theta_1 \varepsilon \frac{D}{c}K \geq 0 \quad (13)$$

An imaginary value of the velocity θ means that propagation is impossible. So the value of curvature K which transforms inequality (13) to an equality is the critical value of curvature $K = K_{cr}$

$$K_{cr} = -\frac{c}{D} \left[(\theta_0 - \theta_1 \varepsilon) + 2\sqrt{-\theta_0 \theta_1 \varepsilon} \right] \quad (14)$$

The expression under radical in eqn. (14) is always positive because $\theta_1 < 0$ (θ decreases with the increase of ε). Substituting K_{cr} in eqn. (12), provide the corresponding value of the critical propagation velocity:

$$\theta_{cr} = \left(\theta_0 + \theta_1 \varepsilon + \frac{D}{c}K_{cr}\right) \frac{1}{2} \quad (15)$$

Eqn., (12), (14), and (15) give the required relationship between the propagation velocity and the wave front curvature, but these are in terms of the velocity components θ_0 and θ_1 . It is extremely difficult, if not impossible, to find the relationships between these velocity components and the parameters of most mathemati-

cal models of cardiac cells. An exception is the simplified FN model for which approximated explicit expressions were found [Zykov 1987] to be:

$$\theta_0 = \sqrt{4 \frac{G_f}{1+d^2}} \quad (16)$$

$$\theta_1 = \frac{\lambda^2 G_s}{4(1-E_{th})G_f^2 \theta_0} \left[1 - 3E_{th} - \frac{2\theta_0 \lambda}{\pi G_f} - \frac{\theta_0^2 (1-E_{th})}{\lambda^2} \right] \quad (17)$$

Here: $d = -\frac{\pi}{\ln\left(\frac{1}{E_{th}} - 1\right)}$, $\lambda = \sqrt{4G_f - \theta_0^2}$

The results of the calculation of θ (K) for the FN model with standard parameters values obtained by Zykov [17] from eqn. (12) and using eqn. (16) and (17) are shown as dots in Fig. 1. These data confirmed that analytical estimates give satisfactory accuracy for the FN simplified model.

2.2 Anisotropic tissue

In the case of anisotropic tissue such as heart muscle tissue in a normal state, the ratio of diffusion coefficients in the directions of fiber transverse axis to the fiber longitudinal axis is in the range 1:2 to 1:10. For a diseased myocardium it can reach values of 1:20 and greater. If x coincides with the longitudinal axis, $D_x > D_y$. The FN equations for this case take the form

$$D_x \left(\frac{\partial^2 E}{\partial x^2} + \frac{D_y}{D_x} \frac{\partial^2 E}{\partial y^2} \right) = c \frac{\partial E}{\partial t} - F(E) + I - I_{st}$$

$$\frac{\partial I}{\partial t} = \varepsilon(E)(G_s E - I)$$

Introducing the transformation $y = y^* \sqrt{\frac{D_y}{D_x}}$, one can reduce this case to:

$$\left(\frac{\partial^2 E}{\partial x^2} + \frac{\partial^2 E}{\partial y^{*2}} \right) = c \frac{\partial E}{\partial t} - F(E) + I - I_{st} \quad (18)$$

$$\frac{\partial I}{\partial t} = \varepsilon(E)(G_s E - I) \quad (19)$$

Therefore, all the results described in 2.1 can be applied for this as well. The differences from the isotropic case lie in the speed of propagation in the x and y directions and the form of stationary propagated waves. For example, a rectilinear

wave will propagate in y direction with a velocity $\theta_y = \theta_x \sqrt{\frac{D_y}{D_x}}$. When the excitation stimulus is applied to a small circular area, the generating wave has an elliptical form instead of a circular form as in isotropic tissue. As shown below, the anisotropy of the restricted area of the tissue introduces new and very important properties for propagation along narrow paths.

3. The border tissue properties and the form of wave front inside the narrow paths

The narrow paths border tissue properties, as already mentioned, can be divided into three groups: connective tissue with zero current flow through it (zero flux boundary condition for PDE), low excitable tissue, and in a limit case fully unexcitable tissue. The last two properties of border tissue can be associated with patchy infarct and its further development in the course of ischemia. They can be interpreted as an increase of the cell's threshold level. The properties of tissue with high coupling or gap resistance developed in the presence of ischemia can, as a first approximation, be reduced to the first type of border tissue properties.

The form of the wave front can be defined as a function $\alpha = f(s)$, where α is the angle of the tangent of the front of the wave at a point s taken on the chosen equipotential $E = \text{const}$. This angle is measured in respect to the Cartesian coordinate x (see Fig. 2) and can be expressed in terms of the components of $\text{grad } E$ in the direction of current flow, which is normal to the front of the wave at all points. Therefore $\tan \alpha = \frac{\partial E}{\partial x} / \frac{\partial E}{\partial y}$. We now apply these results to estimate the form of the wave front and its curvature inside the narrow paths.

For the border tissue of zero flux type, the component of $\text{grad } E$ along the y axis $\frac{\partial E}{\partial y} = 0$ at all points on the border, and the angle of the tangent to the wave front at all points of the border must be $\pi/2$. The wave front is rectilinear (see Fig. 3a) with a curvature $K = 0$.

For the case when the borders of narrow paths consist of unexcitable tissue, it is possible to assume that the cells of such tissue are held at the rest potential so that the $\text{grad } E$ component $-\frac{\partial E}{\partial x}$ is equal zero at all points of the border, and angle α equals zero at that points. Inside the narrow path this component of $\text{grad } E$ and the angle α increase until they reach maximum values: $\text{grad } E$ and $\alpha = \pi/2$ at the

midpoint of wave front. It is therefore reasonable to approximate the wave front inside a narrow path as a semi-circle with a radius equal to $W/2$ and a curvature $K = 2/W$.

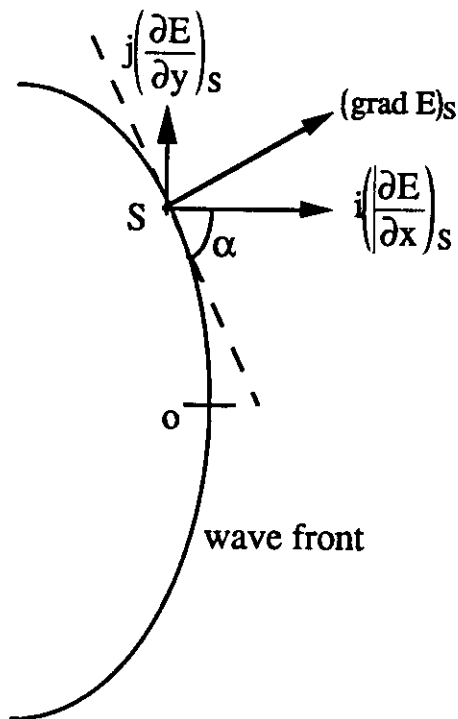


Figure 2. Wave front shape and the components of grad E

When the excitability of the border tissue has some intermediate values, the angle of tangent at the border points is determined by the ratio of the corresponding components of grad E. Because the path is narrow, we can approximate the wave front as a part of a circle with radius $R_b = W/2 \cos \alpha_b$ and curvature $K_b = 1/R_b$

$$K_b = \frac{2}{W} \cos \alpha_b = \frac{2}{W} \frac{1}{\sqrt{1 + \operatorname{tg}^2 \alpha_b}}; \operatorname{tg} \alpha_b = \left(\frac{\partial E}{\partial x} \right)_b / \left(\frac{\partial E}{\partial y} \right)_b \quad (20)$$

Similarly, for any point "i" on the wave front the curvature is found to be

$$K_i = \frac{2}{W_i} \cos \alpha_i = \frac{2}{W_i} \frac{1}{\sqrt{1 + \operatorname{tg}^2 \alpha_i}}; \operatorname{tg} \alpha_i = \left(\frac{\partial E}{\partial x} \right)_i / \left(\frac{\partial E}{\partial y} \right)_i \quad (21)$$

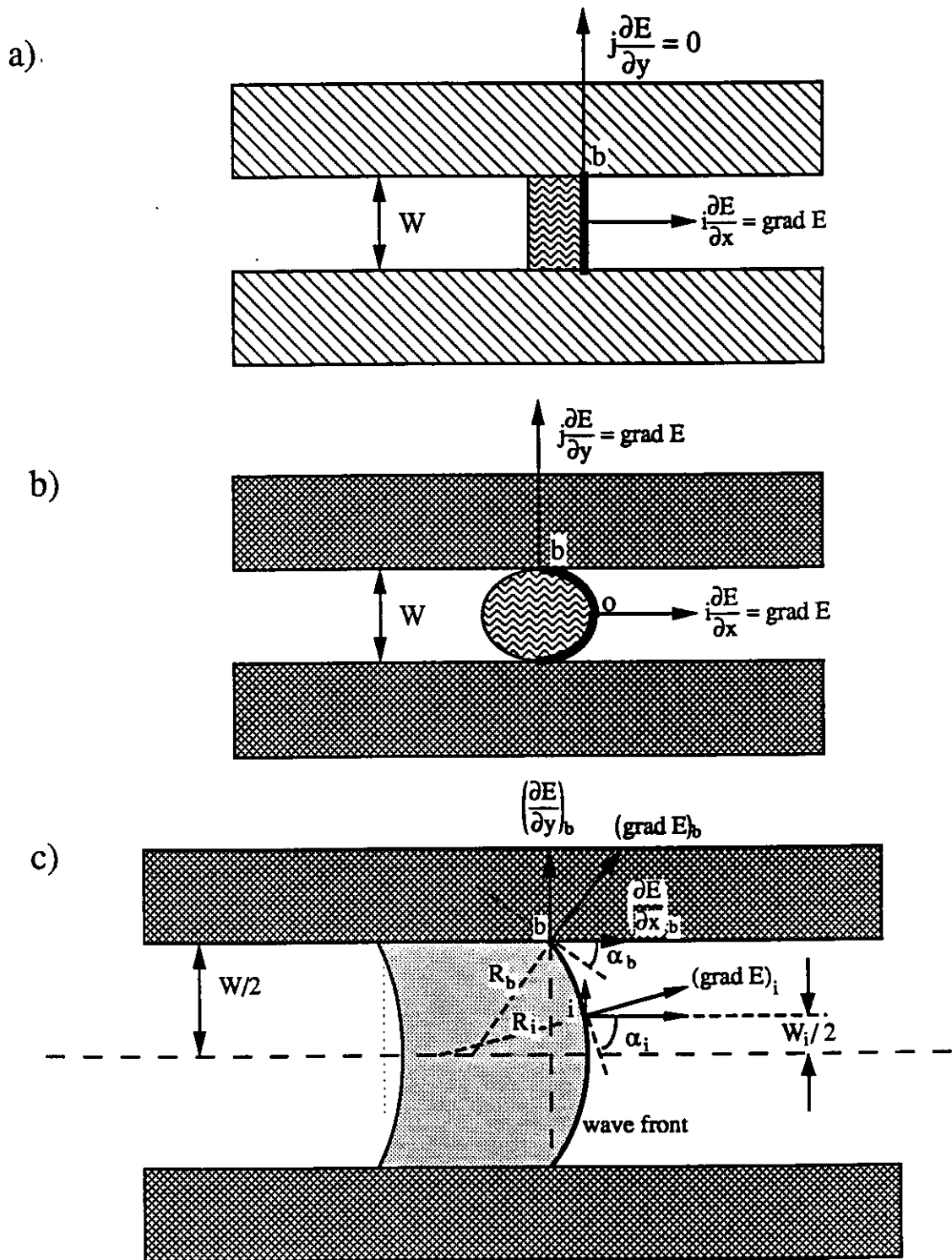


Figure 3. Shapes of wave fronts inside narrow paths with border tissue of different properties. a. Rectilinear wave front inside the narrow path with border tissue of "zero flux" type, $K = 0$. b. Semicircular wavefront inside narrow path with unexcitable border tissue, $K = W/2$. c. Wave front inside narrow path with low excitable

$$\text{border tissue, } K_i = \frac{1}{W_n/2 + (L - L_i) \text{tg } \beta} \cos \alpha$$

Fig. 3 a,b,c. show all the geometric constructions which were used to derive these formulae. The grad E components necessary to determine the angle α_i can be obtained during computer simulation for a particular tissue model at any points on the wave front.

4. Waves propagation along narrow paths with zero flux border tissue

Undamped wave propagation can be initiated by the application of above-threshold excitation to one end of the infinite length path, or by application of two excitation stimuli at appropriately chosen times and sites of application for closed loop configurations (Quan and Rudy [18]). Due to the peculiarity of the boundary conditions, the front of the propagated waves must be perpendicular to the borders at all points. Therefore, the waves with rectilinear fronts will propagate with constant velocities $\theta_{r,l}$ independent of the widths of the narrow paths. In the limit, when the width of the path is equal to the diameter of the cell we come to the case of purely one dimensional propagation, which has been considered in large number of a publications.

The case when the widths of narrow paths increase smoothly or abruptly at the end opposite to that of the excitation application (see Fig. 4a) is of a special interest. By changing the value of the angle β from zero to $\pi / 2$, it is possible to realize a continuous transfer from a narrow path with parallel borders to tapered shape borders with expanding openings. The limit when $\beta = \pi / 2$ corresponds to the abrupt opening of the narrow path to the unrestricted righthalf - plane of the normal excitable tissue. Since the propagated wave front must be perpendicular to the borders at all points, one can come to the conclusion that the wave front at the points "a-a" of the expanding borders can be considered as a first approximation to be arcs of the circles. The simple geometric drawing, shown on Fig. 4a, gives:

$$R=W/2\sin\beta \text{ or } K=1/R=2\sin\beta/W \quad (22)$$

Here: R - radius of wave front at the pathway opening;

W - width of the pathway with parallel borders;

β - angle of border inclination;

K - curvature of the wave front

Equation (22) specifies a family of sinusoidal curves of amplitude $A = 2/W$ and is correct for all points "x-x" on the border of a tapered opening. It is necessary only to substitute in eqn. (22) the value of W at the points "x-x" (see Fig. 4a).

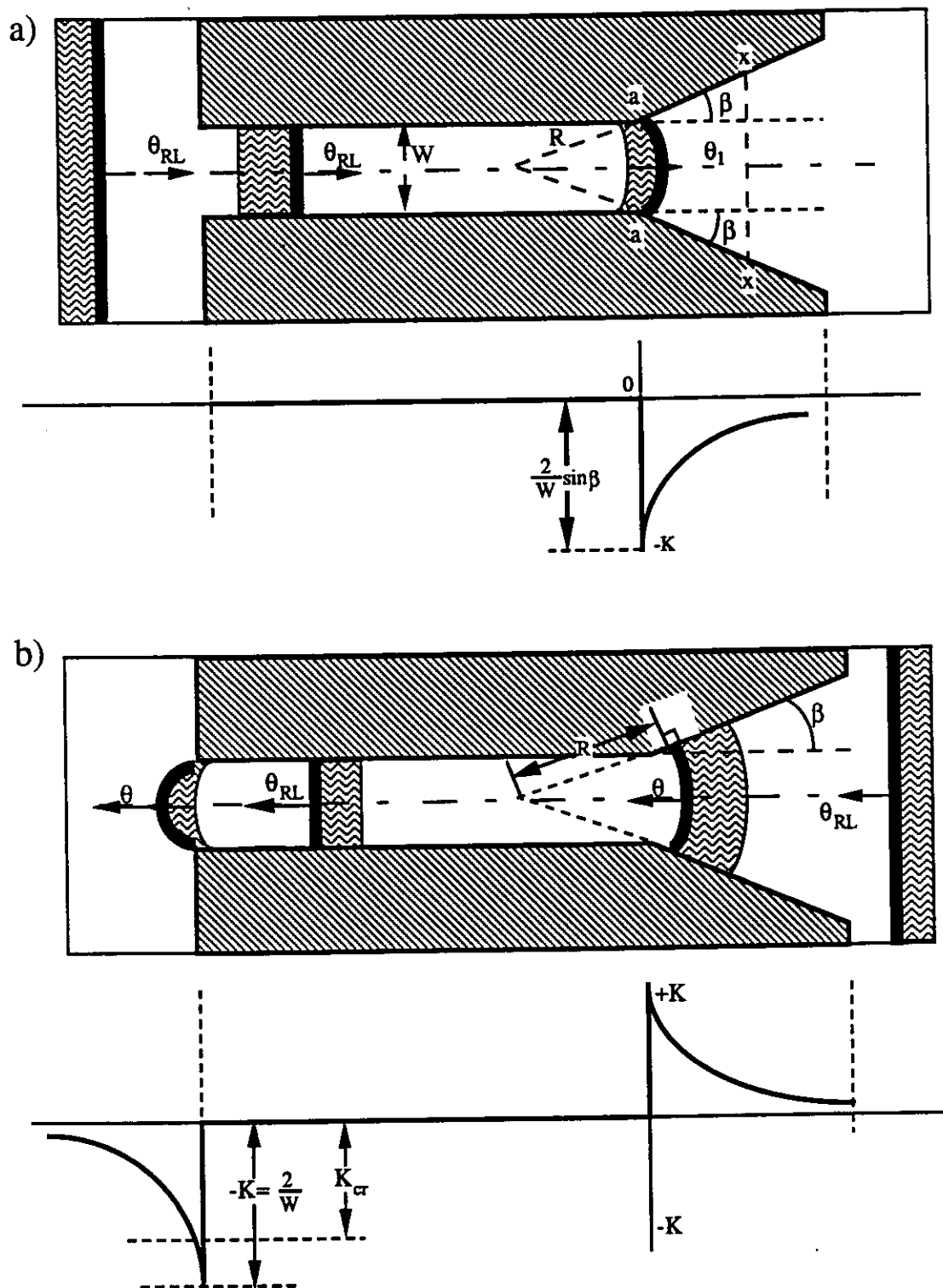


Figure 4. Waves propagation along narrow pathways with border tissue of "zero flux" type: a. The wave passes when a rectilinear stimulus is applied at the left side of a narrow pathway; b. The wave dies out when the stimulus is applied at the right side of a narrow pathway.

As discussed above there exists a critical value of wave front curvature above which propagation becomes impossible, i.e there is a propagation block. Physically this means that the excited cells (source) do not transmit enough electrical current to the neighboring nonexcited cells (sink) for them to reach the excitation threshold value. This critical value depends on the type of the selected cell model and its parameters values. The direct measurement of critical wave curvature is very difficult in physiological experiments. Computer simulation requires a comparatively large amount of calculations which grow with the complexity of the model. Eqn. (22) permits us to measure the width of the narrow pathway instead of the wave front curvature in order to obtain the critical value of front curvature. Indeed, for $\beta = \pi / 2$, $K = 2 / W$. By changing the width of the narrow pathway during computer simulation, one can find the $W=W_{cr}$ at which propagation through the opening becomes impossible. This approach can be used for different types of the mathematical models, for tissue cultures and pieces of real tissue. The similarity of the results obtained using real tissue and the mathematical model can serve as an indication of the fidelity of this model in reproducing the propagation properties.

The values for K_{cr} obtained by Zykov [17] for the FN model using an approximate formula and repeated solution of the original equation ($K_{cr} = - 0.79$) and that using our approach ($K_{cr} = - 0.83$) are in close agreement.

Let us consider the configuration shown on Fig. 4b where W is chosen so that $W = W_{cr}$ and $\beta = \pi / 2$ (left opening). When the wave propagates from left to right, its front curvature remains equal to zero until it reaches the tapered opening . Here the curvature abruptly changes from $K = 0$ to $K = K_{cr} \sin \beta$ so the wave passes in this direction without obstacle. When wave is initiated to propagate from right to left (Fig. 4b) its front takes on a concave form in the tapered pathway, and the curvature changes from some positive value to zero at the entrance of the narrow path. At the left opening with $\beta = \pi / 2$, the curvature abruptly changes from $K = 0$ to $K = K_{cr}$, and block of propagation occurs. This is a case of unidirectional block.

The addition of another pathway in parallel with the width dimension, provided $K < K_{cr}$ (see Fig. 5), makes reentry possible. When the surviving tissue has APD restitution properties, reentry creation requires an additional time delay between the propagation through a pathway with unidirectional block and a parallel pathway without block. This condition can be realized naturally by the anisotropy of the tissue and an appropriate distance between the pathways. Indeed, Cardinal et.al. [5] have shown that the speed of propagation in the longitudinal fiber

direction is 8 to 10 times greater than in the transverse direction. Therefore, wave propagation in the transverse direction introduces an additional time delay. This occurs when the longitudinal axes of excitable tissue inside the narrow path coincides with that of the pathway. The latter is valid for the majority of real situations (Janse and Wit [3]). The anisotropy decreases also the critical width of the narrow path which provides the unidirectional block.

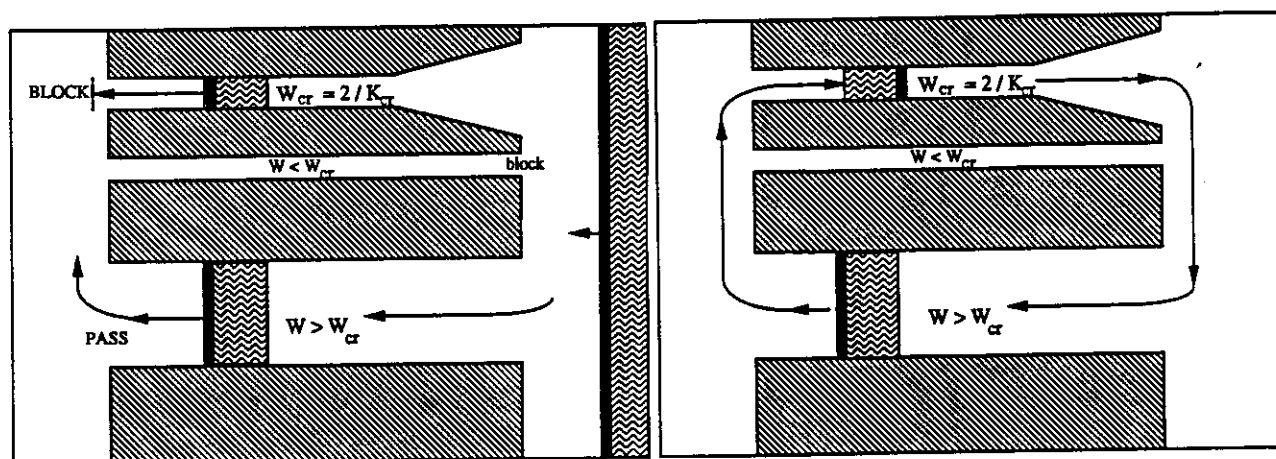


Figure 5. Reentry in tissue with two channels: one with unidirectional block and the other capable of passing the wave in both directions. The border tissue is of "zero flux" type

This effect of anisotropy can be explained by the decrease of current consumption in the transversal direction at the moment when the wave exits the narrow path to the open space of survival tissue. In comparison with the case of isotropic tissue, this leads to a decrease of the wave front curvature outside the narrow pathway. Thus, the anisotropy of the tissue facilitates reentry in the presence of narrow paths with unidirectional block while pronounced APD restitution has the opposite effect.

5. Wave propagation along narrow paths with border formed by low excitable tissue

Let us consider two cases: one when the border tissue is fully unexcitable and another when the excitability of the border tissue has a low value. It was shown earlier that the front of the wave inside the narrow path with unexcitable border tissue can be estimated as a semicircle of radius $R = W/2$ and curvature $K = 2/W$. If the width of the narrow path is $W > W_{cr}$, the waves propagate in both directions. If $W \leq W_{cr}$, the waves die out inside the channel independently of the direction of propagation. Therefore, we conclude that in narrow pathways with unexcitable parallel border tissue unidirectional block is impossible.

Unidirectional block can occur only when the narrow path has the proper tapered shape. Waves propagated from wide end of the tapered channel die out at the narrow end while waves propagated in opposite direction are able to pass through.† This can be explained by the increase of wave front curvature (Kogan et.al. [20]) along the tapered channel toward the narrow end Fig. 6.

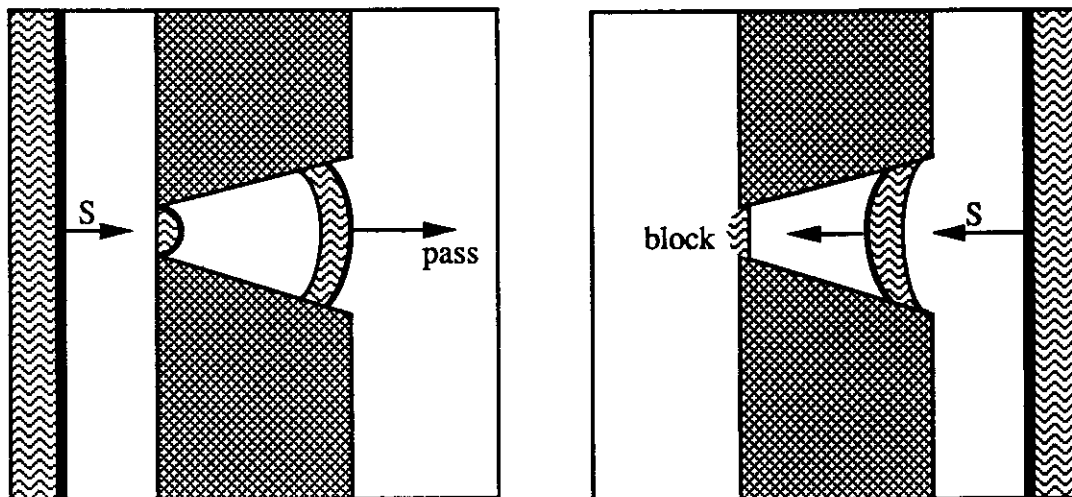


Figure 6. Wave propagation through tapered pathways with borders of low excitable tissue.

If the curvature at this end reaches the critical value, propagation becomes impossible. When a wave propagates toward the wide end of the channel, its curvature changes from zero (rectilinear front) to the maximal value $K = \frac{2}{W_n} \cos\beta$. If this value

† This phenomenon was observed in course of computer simulation by A. Pang and B. Billett see Pang [19].

is chosen so that $K < K_{cr}$, the wave is able to propagate.

The same reasoning can be applied to the case of border tissue with low excitability. Unidirectional block is possible only in a tapered pathway with properly chosen geometry. The expression for curvature at any border points "i" inside the channel (Fig. 7) has a more complicated form:

$$K_i = \frac{1}{W_n/2 + (L - L_i) \operatorname{tg} \beta} \cos \alpha \quad (23)$$

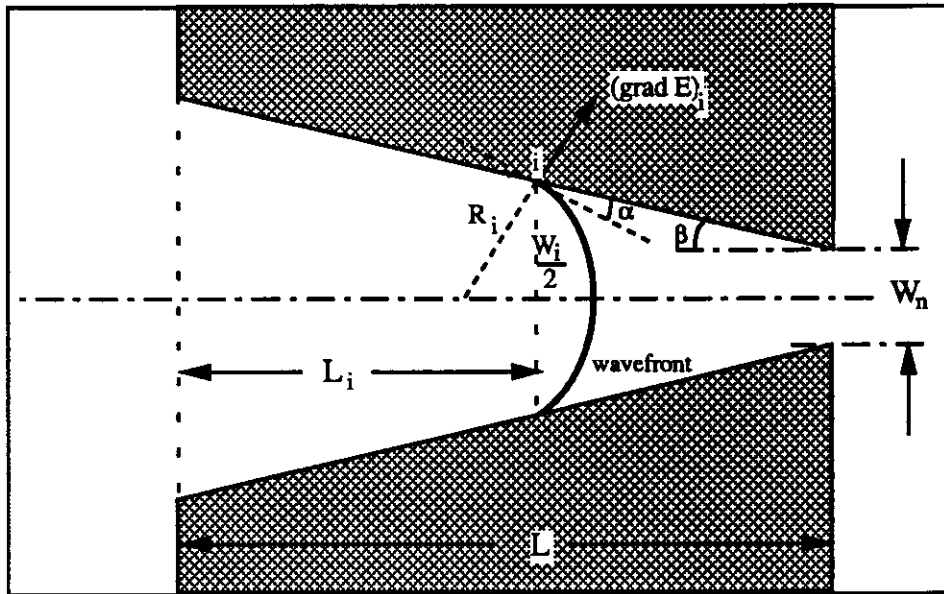


Figure 7. Geometry for the determination the curvature of wave fronts at the borders of low excitable tissue in tapered pathways.

The unidirectional propagation through tapered pathway for both cases of low excitability can be also explained physically in terms of source and sink. However, the wave front curvature concept has the additional advantage of establishing the relationship between the geometry of pathway and internal wave propagation. Reentry can be achieved by the addition, in parallel to the narrow path with unidirectional block, of at least one channel of any form that provide bidirectional or unidirectional propagation (Fig. 8a,b).

APD restitution properties of the tissue inside the narrow path tend to inhibit reentry, while anisotropy of the survival tissue introduces the required time delay for the reentering wave, which provides complete recovery from the previous excitation of the tissue inside the narrow path.

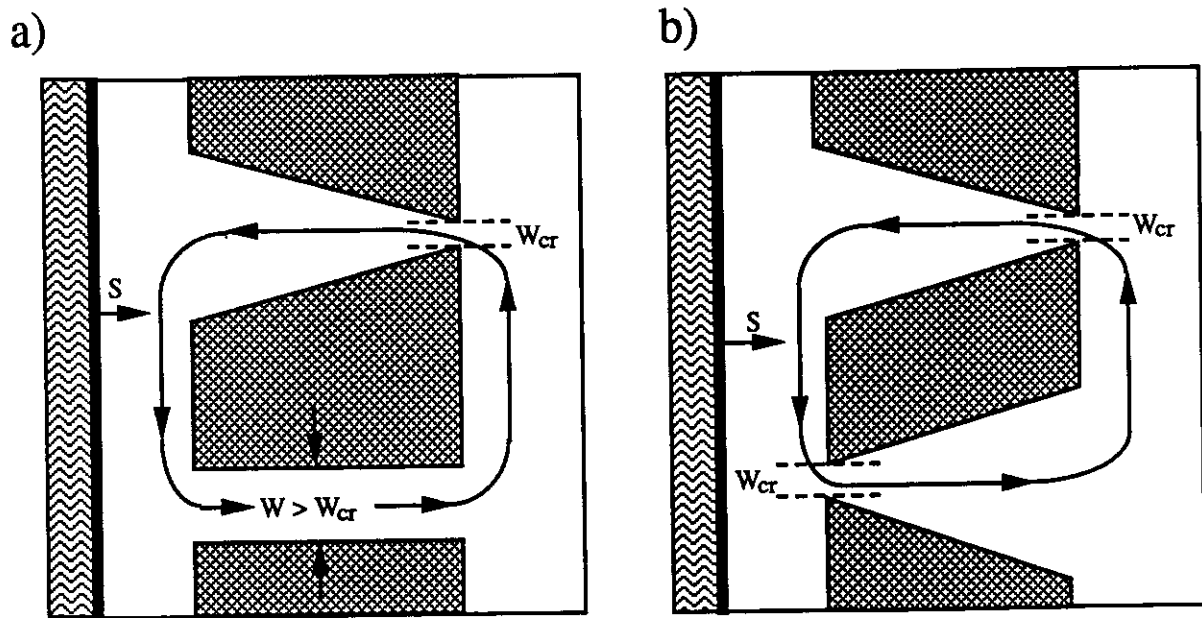


Figure 8. Reentry in tapered pathways with low excitable border tissue: a. Unidirectional block in one channel, b. Unidirectional block in both channels.

The tissue anisotropy also decreases the grad E component in the direction transversal to the fiber and increases it in the longitudinal direction. This increases the curvature of the wave front in the longitudinal direction creating difficulties for the reentering wave to penetrate the narrow end of tapered channel. Therefore, for the case of narrow paths with low excitable border tissue, tissue anisotropy under certain conditions produces a dual effect on reentry - to facilitate and inhibit simultaneously.

Summary of results

1. Narrow paths with zero flux border tissue

- Inside infinite length narrow paths with parallel borders, waves propagate with rectilinear front normal to the borders. The conduction velocity does not depend on the width or the length of the pathway. Wave front curvature is everywhere zero.

- When these pathways have a finite length and an opening on both of its ends, the wave propagates with a rectilinear front only inside the part of the pathway with parallel borders. The wave front and its curvature changes when passing the opening in both directions. At the points at which the curvature reaches the critical value, conduction block occurs. The relationship between the front curvature K and the pathway geometry (opening angle β , width W) is $K = 2 \sin \beta / W$,

2 . Narrow pathways with borders formed of low excitable tissue

- In the limit, when parallel borders are fully unexcitable, the wave propagates or is blocked in both directions as determined by the channel width. The wave front curvature is approximately $K = 2/W$.
- Unidirectional block for low excitable border tissue, is possible only for narrow tapered paths. Under certain conditions, impulses entering from the narrow end of the tapered channel propagate, while impulses entering from the wide end die out.
- For intermediate values of border tissue excitability, the curvature of the wave front inside the tapered channel can be estimated using eqn. (23).

3. Role of APD restitution and tissue anisotropy

- APD restitution properties tend to inhibit reentry. For reentry to occur an increased time delay for wave propagation in the reentry loop is required.
- For narrow paths with zero flux border tissue, tissue anisotropy greatly facilitates the development of reentry (introduces natural delay) and at the same time expands the range of path width (in the direction of smaller width) for which unidirectional block and reentry are possible.
- For narrow paths with low excitable tissue, the tissue anisotropy produces a dual effect on reentry occurrence (to facilitate and inhibit simultaneously).

Conclusion

We found that the geometry and border conditions for narrow pathways inside regions of homogeneous tissue have several important effects on impulse propagation:

1. In homogeneous tissue, pathway geometry alone can lead to unidirectional block and slow conduction velocity.
2. Border conditions markedly alter the effects of the pathway geometry.
3. Reentry can occur entirely due to the effects of pathway geometry and border conditions provided the following necessary and sufficient conditions are fulfilled:

- Existence of at least one channel with unidirectional block of wave propagation
 - Existence of at least one additional channel with unidirectional or bidirectional wave propagation connected in parallel with the first one by a region of vital tissue
 - The existence of time delay in propagation through a vital tissue in the direction normal to the longitudinal fiber axis
4. The concept of wave front curvature used in the present study allows us to obtain the quantitative relationships between the wave front curvature inside narrow pathways, the geometry of the pathways and their border properties.

In future studies we will extend these results to the cases of rough borders and 3-D narrow paths.

ACKNOWLEDGMENTS

The authors gratefully acknowledge Dr. William Stevenson of the UCLA Medical Center for drawing our attention to the problem of excitation wave propagation in narrow paths. Research in the use of massive parallelism for system simulation in the UCLA Computer Science Department is supported in part by the NASA/Dryden Research Center under Grant NCC 2--374 and NSF Grant BBS 87--14206.

REFERENCES

1. Winfree A.T. Vortex Action Potential in Normal Ventricular Muscle (Ed. Jalife J.), pp 190-207. Mathematical Approach to Cardiac Arrhythmias. Annals of the New York Academy of Sciences, vol 591, The New York Academy of Sciences, 1990.
2. Ideker R. E., Frazier D.W., Krassowka W. Shibato N., Chen P.S. Kavanagh K.M., and Smith W.M. Experimental evidence for Autowaves in the Heart New York Academy of Sciences, vol 591, pp 208 - 218, The New York Academy of Sciences, 1990.

3. Janse M.J. and Wit A.L. Electrophysiological Mechanisms of Ventricular Arrhythmias Resulting from Myocardial Ischemia and Infarction, *Physiol. Rev.*, v 69, pp 1049- 1169, 1989.
4. De Bakker J.M.T. , Coronel R. , Tasseron S. , Wilde A.A.M. , Orthof T. , Janse M.J. , Van Capelle F.G.L. , Bekker A.E. , Jambroes G. Ventricular Tachycardia in the Infarcted, *Langendorf - Perfused Human Heart: Role of the Arrangement of Surviving Cardiac Fibers*, *JACC*, Vol 15, pp 1594- 1607, 1990.
5. Cardinal R. , Vermulen M. , Shenasa M. , Roberge F. , Page P. , Helie F. Anisotropic Conduction and Functional Dissociation of Ischemic Tissue During Reentrant Ventricular Tachycardia in Canine Myocardial Infarction, *Circulation.*, v 77, pp 1162-1176, 1988.
6. Wit A.L. Dillon S.M. Coromiles J. Soltman A.E., and Waldecker B. Anisotropic Reentry in the Epicardial Border Zone of myocardial Infarcts. *Mathematical Approach to Cardiac Arrhythmias* (ed. Jalife J.). *Annals of New York Academy of Sciences*, vol 591. pp 62 - 74, The New York Academy of Sciences, 1990.
7. Dillon S.M. , Allessie P.C. , Ursell P.C. and Wit A.L. Influence of Anisotropic Tissue Structure on Reentrant Circuits in the Epicardial Border Zone of Subacute Canine Infarcts, *Circ. Res.*, Vol 63, pp182 - 206, 1989.
8. Spach M.S. , Dolber P.C. , and Hudlage J.F. Properties of Discontinuous Anisotropic Propagation at a Microscopic Level. *Mathematical Approach to Cardiac Arrhythmias* (ed. Jalife J.). *Annals of New York Academy of Sciences*, vol 591, pp 62 - 74, The New York Academy of Sciences, 1990.
9. Rudy Y. and Quan W. A Model Study of the Effect of Discrete Cellular Structure on Electrical Propagation in Cardiac Tissue. *Circ. Res.*, Vol. 61 ,No 6, 1987.
10. Kogan B.Y. , Karplus W.J. , Pang A.T. Simulation of Nonlinear Distributed Parameter Systems on the Connection Machine, *Simulation*, vol 55, pp 271-280, 1990.
11. Kogan B.Y. , Karplus W.J. , Billett B.S. , and Pang A.T. , Karagueuzian H.S. , and Khan S.S. The Simplified FitzHugh - Nagumo Model With Action Potential Duration Restitution: Effects on 2-D Wave Propagation, *Physica D*, 206, pp (in press), 1991.

12. Ashour S.S., and Hanna O.T. A New very Simple Explicit Method for the Integration of Mildly Stiff Ordinary Differential Equations, *Computers chem. Engng*, Vol. 14, No. 3, pp267 - 272, 1990.
13. Zykov V.S. Analytic estimate of the dependence of excitation wave velocity in a two dimensional excitable medium on the curvature of its front, *Biofizika* 25(5), 1980.
14. Tyson J.J. , Keener J.P. Singular Perturbation Theory of Traveling Waves in Excitable Media, *Physica D*, 32, pp 327-361, 1988.
15. Hodgkin A.L. and Huxley A.F. A quantitative description of membrane current and its application to conduction and excitation in nerve. *J. Physiol.*, 117, 500, 1952.
16. Nagumo J, Arimoto S. and Yoshizava S. An active pulse transmission line simulating nerve axon. *Proc IRE*, 50, 2061, 1962.
17. Zykov V.S. *Simulation of Wave Processes in Excitable Media*, Manchester University Press, 1987.
18. Quan W. and Rudy Y. Unidirectional Block and Reentry of Cardiac Excitation: A Model Study. *Circ. Res.*, Vol 66, no 2, 1990.
19. Pang A.T. *On simulating and Visualizing Nonlinear Distributed Parameter Systems Using Massively Parallel Computers*, PhD Thesis, UCLA, { { 1990.
20. Kogan B.Y. ,Karagueuzian H.S. , Karplus W.J. , Khan S.S. , Billett B.S. , Pang A.T. , Stevenson W.G. Unidirectional Conduction Block Caused by Variation in Pathway Geometry: A New Mechanism for reentry, *JACC*, vol 17, pp 386 A, 1991.